Small period long period fiber grating with improved refractive index sensitivity and dual-parameter sensing ability

FANGCHENG SHEN[1, 2], CHANGLE WANG[2], ZHONGYUAN SUN[2], KAIMING ZHOU[2, 3], LIN ZHANG[2], AND XUEWEN SHU[1,*]

[1]*Wuhan National Laboratory for Optoelectronics & School of Optical and Electronic Information, Huazhong University of Science and Technology, Wuhan 430074, China*
[2]*Aston Institute of Photonic Technologies, Aston University, Birmingham B4 7ET, UK*
[3]*Xi'an institute of optics and precision mechanics, Chinese Academy of Sciences*
**Corresponding author: xshu@hust.edu.cn*

Received XX Month XXXX; revised XX Month, XXXX; accepted XX Month XXXX; posted XX Month XXXX (Doc. ID XXXXX); published XX Month XXXX

Long period fiber grating with a period of 25 μm is UV inscribed and characterized. A series of polarization dependent dual peak pairs can be seen in the transmission spectrum even only symmetric refractive index modification is introduced. The fabricated grating exhibits a lower temperature sensitivity compared with standard long period grating, and an enhanced refractive index sensitivity of ~ 312.5 nm/RIU averaged from 1.315 to 1.395, which is more than four-fold higher than standard long period grating in this range. The full width at half maximum (FWHM) of the fabricated grating is only about 0.6 nm, allowing for a high resolution sensing. Moreover, the grating period is so small that the attenuation dip corresponding to high order Bragg resonance can also be seen, which can act as a monitor of the unwanted perturbation to realize dual parameter sensing. © 2016 Optical Society of America

OCIS codes: *(050.2770) Gratings (060.2340) Fiber optics components; (060.2370) Fiber optic sensors; (060.3735) Fiber Bragg gratings*

http://dx.doi.org/10.1364/OL.99.099999

Optical fiber sensors based on fiber gratings, including fiber Bragg gratings (FBGs) and long period gratings (LPGs), have attracted considerable attention in the past few decades [1]. Usually, FBG is associated with coupling between counter propagating core modes if not tilted, while LPG is related to coupling from core mode to co-propagating cladding modes. For refractive index (RI) sensing, which is useful in environmental monitoring and biomedical/chemical application, LPG is preferred due to its intrinsic high RI sensitivity, and a large body of works have been published [2]. However, the high sensitivity can be a mixed blessing of LPG, as cross-sensitivity with the unwanted perturbation may be induced, for example, the temperature cross-sensitivity in RI sensing, which is an essential issue that needs to be addressed for reliable RI sensing application. Moreover, despite the large body of works published, previously reported LPG has a typical period ranging from 100 μm to 1 mm [2], LPG with a period below this range, e. g. tens of micrometers, is rarely investigated. X. Shu et al systematically characterized the sensitivity of LPG with a period down to 34 um [3], but the spectral properties are not shown.

The excessively tilted fiber grating (ETFG) is a relatively new type of fiber grating that has a tilt angle around 81 degree [4]. It shows unique polarization-dependent dual-peak pairs (DPPs), and has been successfully employed in fiber laser and sensing application [4-7]. In a recent analysis, the arising of the DPPs is attributed to the degeneracy of cladding modes (TE, TM mode) at high mode order [8], i.e., it's the intrinsic mode properties of the single mode fiber (SMF), rather than the large tilt angle, that is responsible for the distinct DPPs. Note that, since coupling to high order cladding modes can also be realized by a LPG that has a similar axial period to the one of ETFG, such a small period LPG (SP-LPG) is expected to have similar spectrum characteristic, which has not been reported so far to the best of our knowledge. The proposed SP-LPG can serve as a reference to the ETFG that may enable a deeper understanding of coupling mechanism of the DPPs in ETFG, which is not fully understood considering the discrepancy of the number of DPPs remained between the theoretical analysis and experiment [8].

In this letter, we demonstrate the fabrication of small period LPG with a period of 25 μm, the SP-LPG shows an enhanced RI sensitivity and reduced thermo sensitivity. DPPs of the SP-LPG are similar to but not the same with that of ETFG, and the difference is explained. Bragg reflection can also be seen, as the grating period is much smaller than standard LPG, which is useful for dual parameter sensing application to monitor the unwanted

perturbation. Sharing the merits of the ETFG, the proposed SP-LPG can relieve the fabrication complexity of the ETFG as no tilt angle control is required.

In our experiment, a frequency doubled Ar^+ laser (central wavelength = 244 nm) is used for the fabrication. The laser source is focused into the core of the hydrogen loaded SMF by a cylindrical lens. The period of the SP-LPG is determined to be 25 μm by the custom-designed amplitude mask, which is placed close to the SMF. After the inscription, the inscribed structure is annealed at 80 °C for 48 hours to stabilize the inscribed structure. Fig. 1 shows the structure of the SP-LPG observed under the microscope with conventional bright field microscope technique, where periodic RI perturbation can be seen in the core of the SMF.

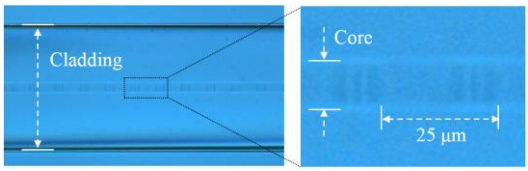

Fig. 1 Microscope image of the inscribed structure, where RI perturbation with a period of 25 μm can be seen.

The transmission spectrum of the SP-LPG measured with an un-polarized light is shown in Fig. 2a, where series of DPPs can be clearly seen. It is worth noting that, in the SP-LPG, the strength of the DPPs is different (strong DPPs and weak DPPs appear alternately), while in the ETFG, the DPPs have almost the same strength. To determine which cladding modes the resonances correspond to, the relationship between the grating period and the wavelength of the strongest coupling is simulated using the same model reported in [8], where the cladding mode index is calculated approximating the fiber as a coreless rod surrounded by air. In the simulation, only cladding modes with the lowest azimuthal order are taken into account, because for untilted grating, coupling to cladding modes with high azimuthal order should be zero for a circularly symmetric RI perturbation [9].

The simulated result is shown in Fig. 2b, where mode index difference between TE and TM mode can be seen. Comparing Fig. 2a with Fig. 2b, it can be found that a good agreement between the experiment and simulation results has been achieved, indicating that the two strong DPPs result from the coupling to the lowest azimuthal order cladding modes with a radial order of 33 and 34, respectively. Discrepancy in the resonant wavelength may result from the approximation used here, and the omission of the UV induced average RI change also lead to some deviation. For the weak DPPs, we believe it generated from the coupling to cladding modes with high azimuthal order, which should be zero theoretically but, for the UV-inscribed SP-LPG concerned here, the index perturbation is not perfectly symmetric since the inscription laser decays when it transmits across the fiber, consequently, the DPPs related to coupling to high azimuthal order cladding modes can be generated, but are very weak.

In contrast, coupling to high azimuthal order cladding modes is significantly enhanced in the ETFG due to the large asymmetry introduced by the excessively tilted grating plane, thus, the strength of the ETFG DPPs is much more uniform. The number of ETFG DPPs given by the experimental results is more than that of the theoretically calculated ones [8], because only cladding modes with the lowest azimuthal order are considered in the simulation, while the coupling to high azimuthal order cladding modes causes the appearance of extra DPPs in the experiment.

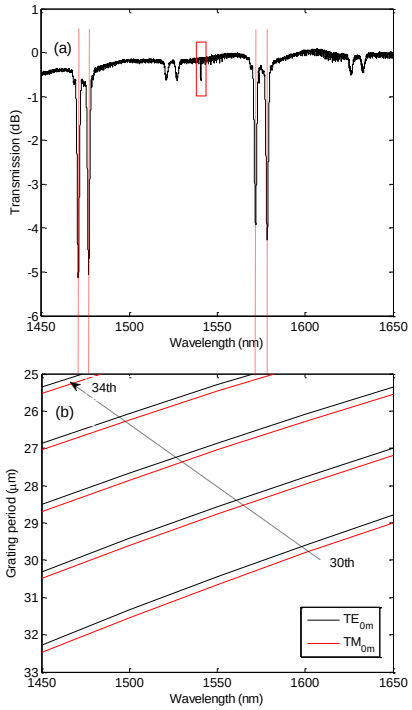

Fig. 2 (a) Transmission spectrum of the SP-LPG probed with un-polarized light, where DPPs with different strength can be seen. (b) Simulated grating period versus the resonant wavelength with TE (black line) and TM (red line) mode for radial order m = 30 to 34.

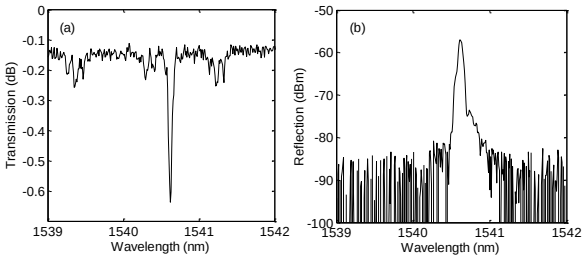

Fig. 3 (a) Zoomed transmission spectrum around 1540.5 nm (indicated by red rectangle in Fig. 2a), where the 47th order Bragg resonance can be seen, and the smaller dips corresponding to cladding mode coupling. (b) Reflection spectrum of the 47th order Bragg resonance.

The grating period is so small that, attenuation dip corresponding to high order Bragg resonance can also be seen from Fig. 3a, which shows the zoomed transmission spectrum around 1540.5 nm. For grating with a period of 25μm, the strongest dip corresponds to the 47th order Bragg resonance, and the weak dips are associated with counter-propagating cladding mode coupling. To verify that the strongest dip results from the Bragg resonance, we measured the reflection spectrum of the SP-LPG given in Fig. 3b, where index matching gel is used to eliminate

the unwanted reflection from the fiber end, and an optical circulator is used to collect the reflected light. The additional Bragg resonance in an LPG spectrum, as previously achieved by the sampled FBG [10], is useful in dual parameter sensing, since the unwanted perturbation that the LPG is sensitive to, need to be monitored to realize reliable sensing application. The strength of the Bragg resonance is relatively weak, which can be enhanced by further reducing the grating period, or by introducing a stronger RI modulation, for example, using femtosecond laser inscription.

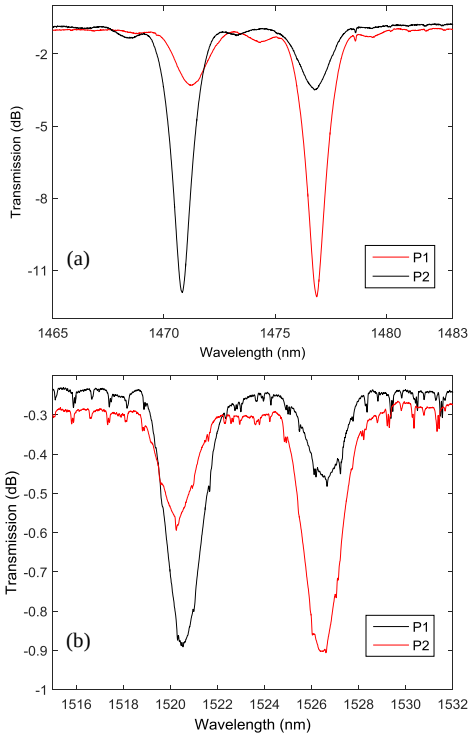

Fig. 4 Polarization dependence of: (a) the strong DPP around 1475 nm, and (b) the weak DPP around1524 nm in transmission.

To characterize the polarization dependency of the DPPs, a polarizer followed by a polarization controller are used to control the polarization state of the light entering the SP-LPG. Fig. 4a shows the zoomed transmission spectrum of the strong DPP around 1475 nm, where orthogonally polarized light is used. We can see that, with a proper choice of the polarization, one of the peak is suppressed to be around 2 dB, while the other is fully exited with a ~11 dB attenuation. Fig. 4b depicts the polarization dependence of the weak DPP around 1524 nm, where a high polarization dependence is also shown: one of the peak can be suppressed to be ~0.5 dB, and the other is enhanced to be ~0.9 dB when the polarization is properly controlled. Note that such a strong polarization dependence is realized with an almost symmetric inscription, which means that the polarization dependence is related to the intrinsic mode properties of the SMF rather than the asymmetric RI perturbation, although the asymmetry indeed helps to maintain the polarization state of light transmitting through the grating, and to enhance the coupling to high azimuthal order cladding modes [8].

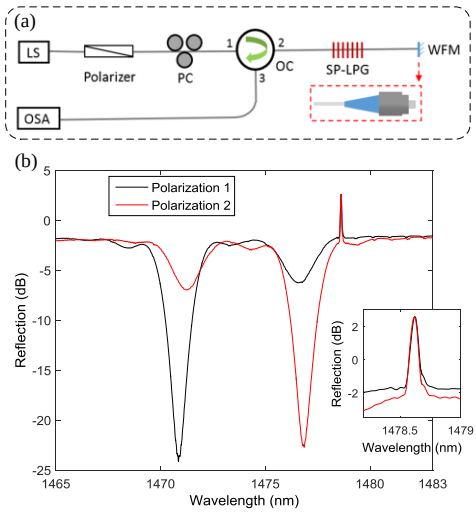

Fig. 5 (a) Experiment setup used to characterize the polarization dependence of the DPP in reflective mode, where: LS: light source, PC: polarization controller, OC: optical circulator, SP-LPG: small period long period grating, WFM: weak reflecting mirror; (b) Measured polarization dependence of the DPP and Bragg resonance around 1475 nm in reflective mode. Inset shows the scaled spectra of the 49th order Bragg resonance.

The polarization dependence of the DPP is also characterized in reflective mode with the experiment setup depicted in Fig. 5a, where a weak reflection mirror (Fresnel reflection of the FC/PC fiber connector here) is used to have a good visibility of the Bragg reflection. The measured results are shown in Fig. 5b, where we can see that the visibility of the 49th order Bragg resonance, which can hardly be seen in the transmission spectrum (Fig. 4a), is significantly improved in this way. The polarization dependence of the DPP is also enhanced since the light passes through the SP-LPG twice. The enhanced polarization dependence can be useful in strength based sensing application, for example, twist sensing [7], as the perturbation-induced strength change is also increased. We can also see from the inset of Fig. 5b that the Bragg resonance is polarization insensitive, indicating a good symmetry of the UV-induced RI modification.

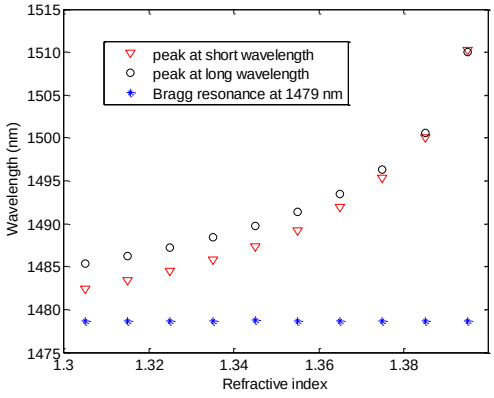

Fig. 6 Variation of the peak wavelength when the SP-LPG is immersed into solution with different RI. The averaged RI sensitivity of the DPP is more than 300 nm/RIU, while the Bragg resonance is insensitive to surrounding RI change.

The sensing potential of the SP-LPG was also evaluated, we immersed the SP-LPG into solutions with different RIs at room temperature, and tracked the wavelength variation of the three resonances shown in Fig. 5b. The SP-LPG was kept straight for all the measurement. It should be noticed that, the full width at half maximum (FWHM) of the fully exited peak of the SP-LPG is only ~ 0.6 nm, which is much narrower than that of normal LPG (20 to 30 nm range for LPG with a period around 550 to 600 μm [11]) and in consequence, allows for a higher resolution measurement. The measured wavelength evolution against RI is shown in Fig. 6, where we can see that the Bragg resonance is insensitive to RI change as expected, and the small variation of the Bragg wavelength may result from the room temperature fluctuation. It can also be seen from Fig. 6 that both peak wavelengths of the DPP increase with the RI, but the wavelength increasing rate of the peak at short wavelength side is higher than the one at long wavelength side, as a result, the wavelength separation between the DPP decreases with an increasing RI. This is consistent with the ETFG, as the mode index difference is related to the RI difference between the cladding and the surrounding environment, which approaches zero as the surrounding RI increases. The wavelength change of peak at long wavelength is ~25 nm when the RI is increased from 1.315 to 1.395, suggesting an averaged RI sensitivity of ~312.5 nm/RIU, which is more than four-fold higher than normal LPG, and two-folder higher than LPG specially designed for enhanced refractive index sensitivity where internal geometric bending is introduced [12].

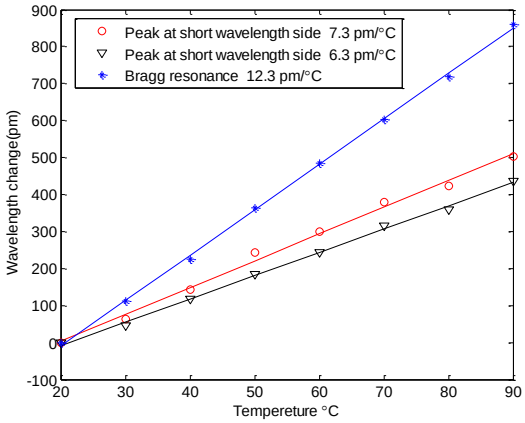

Fig. 7 Variation of the peak wavelength with different temperature. The temperature sensitivity of the DPP is significantly lower than that of the Bragg resonance.

To realize reliable sensing with an LPG based sensor, it is essential to eliminate the cross talk with respect to the unwanted perturbation, such as the temperature cross-sensitivity in RI sensing, which has been previously addressed using a sampled FBG [10], and/or with the help of one more sensing element, for example, an additional FBG as suggested by Patrick et al. [13]. For the SP-LPG considered here, thanks to the much smaller grating period, the co-existed Bragg resonance can act as a temperature monitor to solve the cross-sensitivity problem. Fig. 7 shows the temperature response of the SP-LPG, where the Bragg resonance shows a sensitivity of 12.3 pm/°C, which is comparable with previously reported results, while the temperature sensitivity of the DPP is only 7.3 pm/°C for the peak at short wavelength side, and 6.3 pm/°C for the long wavelength side one. Considering the intrinsic low temperature cross sensitivity of the SP-LPG, the Bragg resonance can also be used to monitor other perturbation if necessary.

In conclusion, long period grating with a much small period of 25μm is fabricated by UV laser in hydrogen loaded single mode fiber, and the fabricated SP-LPG shows a series of polarization dependent DPPs even no polarization related inscription is introduced. The DPPs are similar to but not the same with the ones in ETFG. In the SP-LPG, the strength of the DPPs is different (strong DPPs and weak DPPs appear alternately), while in the ETFG, the DPPs have almost the same strength. Comparison with simulation result suggests that coupling to cladding mode with lowest azimuthal order generates the polarization dependent DPPs in a SP-LPG. The grating period is so small that high order Bragg resonance can also be seen, which can be used to monitor the unwanted perturbation that may deteriorate the sensing accuracy. The SP-LPG shows an improved RI sensitivity that is more than four-fold higher than normal LPG, and a suppressed temperature cross-sensitivity that is even smaller than FBG. Thanks to the significantly reduced FWHM of the SL-LPG attenuation band, a much higher resolution can be achieved. Apart from acting as a highly sensitive RI sensor with an improved resolution and dual-parameter sensing ability, the SP-LPG can also serve as a reference to the ETFG to deepen the understanding of the coupling mechanism, and of the effect of the tilt angle, which is less explored even though quite a lot of experiment works have been reported.

Funding. Wuhan National Laboratory for Optoelectronics Director Fund.

Acknowledgments. FS acknowledges China scholarship Council for financial support, and thanks Dr. Zhijun Yan for the useful discussion.

References

1. A. D. Kersey, M. A. Davis, H. J. Patrick, M. LeBlanc, K. P. Koo, C. G. Askins, M. A. Putnam, and E. J. Friebele, J. Lightwave Technol. **15**, 1442 (1997).
2. S. W. James, and R. P. Tatam, Meas. Sci. Technol. **14**, R49 (2003).
3. X. Shu, L. Zhang, and I. Bennion, J. Lightwave Technol. **20**, 255 (2002).
4. K. Zhou, L. Zhang, X. Chen, and I. Bennion, Opt. Lett. **31**, 1193(2006).
5. C. Mou, P. Saffari, H. Fu, K. Zhou, L. Zhang, and I. Bennion, Appl. Opt. **48**, 3455 (2009).
6. Z. Zhang, C. Mou, Z. Yan, Y. Wang, K. Zhou, and L. Zhang, Opt. Express **23**, 1353 (2015).
7. C. Mou, Z. Yan, K. Zhou, and L. Zhang, Optical Sensors - New Developments and Practical Applications (2014).
8. Z. Yan, H. Wang, C. Wang, Z. Sun, G. Yin, K. Zhou, Y. Wang, W. Zhao, and L. Zhang, Opt. Express **24**, 12107 (2016).
9. T. Erdogan, J. Opt. Soc. of Am. A **14**, 1760 (1997).
10. X. Shu, B. A. L. Gwandu, Y. Liu, L. Zhang, and I. Bennion, Opt. Lett. **26**, 774 (2001).
11. A. M. Vengsarkar, P. J. Lemaire, J. B. Judkins, V. Bhatia, T. Erdogan, and J. E. Sipe, J. Lightwave T. **14**, 58 (1996).
12. F. Chiavaioli, C. Trono, and F. Baldini, Appl. Phys. Lett. **102**, 231109 (2013).
13. H. J. Patrick, A. D. Kersey, and F. Bucholtz, J. Lightwave Technol. 1998, **16**, 1606 (1998).

References with title

1. Kersey A D, Davis M A, Patrick H J, et al. Fiber grating sensors[J]. Journal of lightwave technology, 1997, 15(8): 1442-1463.
2. James S W, Tatam R P. Optical fibre long-period grating sensors: characteristics and application[J]. Measurement science and technology, 2003, 14(5): R49.
3. Shu X, Zhang L, Bennion I. Sensitivity characteristics of long-period fiber gratings[J]. Journal of Lightwave Technology, 2002, 20(2):255-266.
4. Zhou K, Zhang L, Chen X, et al. Optic sensors of high refractive-index responsivity and low thermal cross sensitivity that use fiber Bragg gratings of >80 degrees tilted structures.[J]. Optics Letters, 2006, 31(9):1193-5.
5. Mou C, Saffari P, Fu H, et al. Single- and dual-wavelength switchable erbium-doped fiber ring laser based on intracavity polarization selective tilted fiber gratings.[J]. Applied Optics, 2009, 48(18):3455-9.
6. Zhang Z, Mou C, Yan Z, et al. Switchable dual-wavelength Q-switched and mode-locked fiber lasers using a large-angle tilted fiber grating.[J]. Optics Express, 2015, 23(2):1353-60.
7. Mou C, Yan Z, Zhou K, et al. Optical Fibre Sensors Based on UV Inscribed Excessively Tilted Fibre Grating[M]// Optical Sensors - New Developments and Practical Applications. 2014.
8. Yan Z, Wang H, Wang C, et al. Theoretical and experimental analysis of excessively tilted fiber gratings[J]. Optics Express, 2016, 24(11).
9. Erdogan T. Cladding-mode resonances in short- and long-period fiber grating filters[J]. Journal of the Optical Society of America A, 1997, 14(8):1760-1773.
10. Shu X, Gwandu B A, Liu Y, et al. Sampled fiber Bragg grating for simultaneous refractive-index and temperature measurement.[J]. Optics Letters, 2001, 26(11):774-6.
11. Vengsarkar A M, Lemaire P J, Judkins J B, et al. Long-period fiber gratings as band-rejection filters[J]. Journal of Lightwave Technology, 1996, 14(1):58-65.
12. Chiavaioli F, Trono C, Baldini F. Specially designed long period grating with internal geometric bending for enhanced refractive index sensitivity[J]. Applied Physics Letters, 2013, 102(23):231109 - 231109-4.
13. Patrick H J, Kersey A D, Bucholtz F. Analysis of the Response of Long Period Fiber Gratings to External Index of Refraction[J]. Journal of Lightwave Technology, 1998, 16(16):1606-1612